Flexible ring polymers in an obstacle environment: Molecular theory of linear viscoelasticity

Balaji V. S. Iyer* and Ashish K. Lele†
Complex Fluids and Polymer Engineering Group, Polymer Science and Engineering Division, National Chemical Laboratory, Pune 411008, India

Vinay A. Juvekar‡
Department of Chemical Engineering, IIT Powai, Bombay 400076, India

(Received 1 March 2006; revised manuscript received 30 June 2006; published 30 August 2006)

We formulate a coarse-grained mean-field approach to study the dynamics of the flexible ring polymer in any given obstacle (gel or melt) environment. The similarity of the static structure of the ring polymer with that of the ideal randomly branched polymer is exploited in formulating the dynamical model using aspects of the pom-pom model for branched polymers. The topological constraints are handled via the tube model framework. Based on our formulation we obtain expressions for diffusion coefficient D, relaxation times τ, and dynamic structure factor $g(\mathbf{k},t)$. Further, based on the framework we develop a molecular theory of linear viscoelasticity for ring polymers in a given obstacle environment and derive the expression for the relaxation modulus $G(t)$. The predictions of the theoretical model are in agreement with previously proposed scaling arguments and in qualitative agreement with the available experimental results for the melt of rings.

DOI: 10.1103/PhysRevE.74.021805 PACS number(s): 83.80.Sg, 83.10.Kn, 83.60.Bc

I. INTRODUCTION

DNA often naturally occurs in the ring form (plasmid DNA) and is characterized by the technique of gel electrophoresis [1]. Although the technique has been widely used, the dynamics of plasmid DNA through a gel environment is not well understood. This is because of complications that arise in the study of electrophoretic mobility of a plasmid DNA molecule due to its semiflexible and polyelectrolytic nature. A flexible ring polymer in any given environment is a convenient model system to start with for understanding the mobility of molecules like DNA [2]. The development of a framework for studying the dynamics of flexible ring polymers is thus of considerable importance.

The rheological response of a polymeric system is governed to a considerable extent by the macromolecular topology. We expect that this is a consequence of the influence of topological aspects on static and dynamic behavior at a molecular level. Topological constraints that arise in a polymeric system can be considered to be of two types, viz., internal and external, the former corresponding to the macromolecular architecture and the latter to the confinement of the polymer effected due to the presence of obstacles in its environment. The study of rheological response on the basis of molecular theory requires the formulation of frameworks that can capture the influence of both internal and external topological constraints.

The tube model framework has been the most successful phenomenological framework for handling external topological constraints [3]. In the case of linear polymer chains, an uncomplicated static structure not influenced by the presence of obstacles in the environment makes it easier to fit it into the tube model framework. The associated reptation dynamics studies have enabled a better understanding of the viscoelastic response of the linear polymeric systems on a molecular theory basis [4].

In the case of other structures such as star, branch, and rings, there are two complications that arise. First, the static structures are sufficiently complex and in the case of rings the static structure is influenced by the presence of obstacles [5]. Second, for studying dynamics one has to come up with some ingenious conceptualization, like that of the pom-pom model [6] for branched polymers, to fit it into a tube model framework. In the case of rings, the absence of free ends, which play an important role in the reptation relaxation mechanism for linear chains, leads to concerns regarding the application of reptation dynamics for ring polymeric systems [7]. In this paper we develop a framework, called the pom-pom ring (PPR) framework, inspired by the pom-pom model, for studying the dynamics of ring polymers in a fixed obstacle (FO) environment. Further, we use this framework to understand the linear viscoelastic response of the ring polymers in any given obstacle (gel or melt) environment.

We restrict our attention to unknotted ring polymers in the presence of obstacles around them. The obstacle environment can be either a fixed obstacle (gel) or a moving obstacle (melt). Viscoelastic measurements have been done for the melt of rings by two groups [7–9]. The main difficulty in these experiments was the presence of linear contaminants and the probable presence of knotted structures of rings and their influence on the viscoelastic response. Detailed experiments by Roovers *et al.* [7] on ring-linear polymer blends indicate the strong influence of the presence of linear chains on the viscoelastic response of the system. There are opposing viewpoints regarding the influence of the presence of knots on the statics and dynamics. McKenna *et al.* [8] argue that the presence of knotted rings can affect the viscoelastic response, while Roovers *et al.* [7] consider that there is no need to invoke the influence of knots in order to explain the

*Also at Department of Chemical Engineering, IIT Powai, Bombay 400076, India.
†Electronic address: ak.lele@ncl.res.in
‡Electronic address: vaj@che.iitb.ac.in

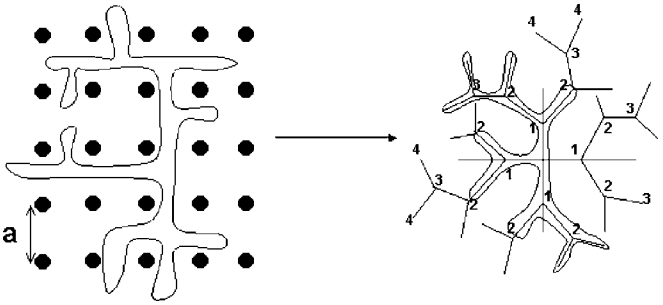

FIG. 1. Cayley tree mapping for a ring polymer.

viscoelastic response of the ring melt. We do not invoke the knotted picture and its influence on statics and dynamics in the framework directly in this paper. Although the knot picture is not directly invoked in the formulation of the framework, it is flexible enough to accommodate changes in static structure and the associated change in dynamics.

In Sec. II we develop, based on physical arguments, a framework for studying the dynamics of ring polymers in a FO environment. We propose a coarse-grained model for a modified primitive chain and describe the salient features related to its dynamics. In Sec. III, we utilize the framework developed in Sec. II and a coarse-grained modified Rouse model to derive expressions for the self-diffusion coefficient, relaxation time, and dynamic structure factor. In Sec. IV we deal with the linear viscoelastic response of the system composed of rings in a FO environment and derive the expression for the relaxation modulus in the linear viscoelastic regime. In Sec. V we extend the results of Sec. IV to that of the melt of rings and compare our theoretical predictions with the experimental results of Roovers [7].

II. POM-POM RING FRAMEWORK

An ideal flexible ring polymer, with Kuhn length b, takes a collapsed conformation in a FO environment with an obstacle of linear dimensions a, when $b<<a<<R_g$ [5]. The conformation of the ring is obtained using a Cayley tree mapping of the obstacle environment followed by forcing a closed random walk on the Cayley tree lattice (Fig. 1). The characteristic length scale for a closed random walk of N steps on a Cayley tree lattice is of order $N^{1/2}$. The resulting conformation is known as a lattice animal or lattice tree structure and resembles that of a randomly branched polymer [5]. The mean-square radius of gyration, R_g, of a ring polymer without excluded volume interactions is given by [10]

$$\langle R_g^2 \rangle = \frac{z}{z-2}\frac{\sqrt{2\pi}}{8}a^2\sqrt{N}, \tag{1}$$

where z is the coordination number of the Cayley tree lattice and a is the step size of the lattice. In the case of an excluded volume branched polymer chain it has been shown that the size of the branched polymer is given by $R_g \sim N^{1/2}$, where N is the number of Kuhn segments [11]. This result holds for excluded volume rings [12].

Scaling arguments for the dynamics of rings in a FO environment (gel) have been worked out for both ideal [13] and excluded volume [12] rings. These arguments are based on the kink-diffusion picture proposed by de Gennes [14] wherein a linear polymer diffuses due to the motion of "length defects" or kinks along its contour. The number of kinks in a linear chain is proportional to the contour length of the polymer chain. The diffusion of each kink has a specific contribution towards the center-of-mass motion of the chain.

The approaches for scaling arguments in the case of rings differ in terms of the contribution of each kink towards the center-of-mass motion. Obukhov *et al.* [13] argue that the kink-diffusion mechanism for rings is different from that of linear chains as opposed to Cates and Deutsch [12]. The latter authors propose a linearlike kink-diffusion mechanism in which the diffusion of all kinks along the contour of the chain contribute to the center-of-mass motion, whereas the former authors propose a distinct mechanism for rings in which not all kinks along the contour contribute to the center-of-mass motion. There arise differences in the scaling results due to variations in static configuration as well as due to the distinct mechanism of kink diffusion. For an ideal ring polymer in the FO environment the former's scaling argument yields the diffusion coefficient $D \sim N^{-2}$ and the longest relaxation time $\tau_d \sim N^{5/2}$ while the latter's scaling argument yields $D \sim N^{-5/2}$ and $\tau_d \sim N^3$.

We do intuitively expect that the absence of free ends could cause a local accumulation of kinks and hence is likely to alter the kink-diffusion mechanism on a global level. As a consequence we discuss the Obukhov *et al.* [13] mechanism in detail and follow up our framework formulation based on it. The mechanism of kink diffusion proposed by Obukhov *et al.* [13] hinges on the lattice-tree structure of the ring polymer. The lattice-tree structure is a self-similar structure composed of substructures, viz., trunk, branches, and leaves with the relaxation of different substructures happening at different time scales. In particular, the diffusion of kinks among branches and leaves is fast and causes only local rearrangements without any center-of-mass motion. The diffusion of kinks along the trunk is slower and causes the center-of-mass motion of the polymer chain. The number of kinks contributing to the center-of-mass motion is thus proportional to the contour length of the trunk instead of the entire ring chain. The dynamics of the trunk, the most predominant length scale, governs the longest relaxation times of the system (Fig. 2).

We use the above physical arguments as a basis for dividing the polymer ring into substructures with the dynamics of different substructures coupled in a specific way. In doing this we consider that for a ring of N segments in the FO environment there exists a characteristic length scale, of the order of $N^{1/2}$ segments as per Eq. (1), which constitutes the primary trunk of the lattice-tree structure. The primary trunk of the ring lattice tree can be unambiguously determined [13] and is the most endurable hypothetical structure among the substructures of the ring lattice tree. Further, the leaves and branches of the lattice tree constitute loops that are attached to the primary trunk at loop points, similar to the branches attached to branch points in a branched polymer. The number of loops is proportional to the length of the primary trunk, $\sim N^{1/2}$. On an average a loop would be composed of $N^{1/2}$ segments, which sit on the hypothetical primary trunk

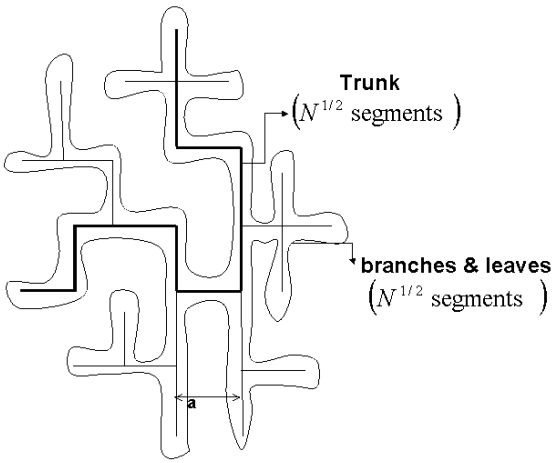

FIG. 2. Trunk, branch, and leaf structures.

(Fig. 3). Given the similarity of the lattice-tree structure to the randomly branched polymer we may now invoke the pom-pom model to describe the dynamics of the ring polymer.

According to the pom-pom model for branched polymers, the branches, if entangled, relax through an arm retraction mechanism, which is the only mechanism allowed by a constricting branch point, and the relaxation times are exponentially dependent on the arm molecular weight [6,15]. Shorter branches, not so entangled, may relax through Rouse modes [16]. The relaxation of the entangled backbone of the branched polymer is constrained by the presence of branch points and can happen only after the relaxation of the branch arms. Thus, the branches add substantially to the friction of the backbone and in the case of the pom-pom model the friction is essentially located at the ends of the backbone [6,16].

In the case of the ring polymer we can consider that the primary trunk of the self-similar lattice animal or lattice tree is entangled with the FO environment, while the loops take a much more collapsed conformation and are hence not entangled and their dynamics is entirely Rouse-type. A subtle difference between a branch point and a loop point is that the segments in the loop can slide into neighboring loops through the trunk, a motion that is not available in branch polymers. However, such sliding of segments between loops is expected to be a rapid process compared to the center-of-mass motion for the trunk and the entire loop has to relax before the trunk segment to which it is attached can diffuse. Thus, the dynamics of the trunk may be affected in a way similar to that of the backbone of the branched polymer. At any point of time for a trunk segment to move, it requires that the loop attached to the specific trunk segment relax completely and allows for the loop point to move. The loops act as frictional constraints for the motion of the trunk.

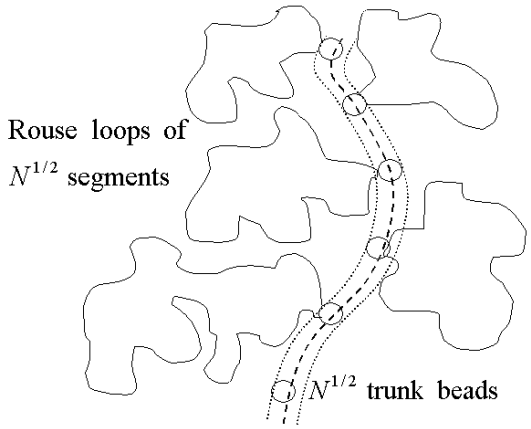

FIG. 3. Model chain for studying dynamics.

On the basis of the physical picture described above, we formulate the PPR framework for studying the dynamics of ring polymers. First, we formulate a modified primitive chain for the ring polymer as follows:

(1) It is constituted by the primary trunk of the lattice animal with a constant contour length given by $L_{trunk}=N^{1/2}b^2/a$.

(2) Each segment of the trunk has attached to it a loop. On an average each loop contains $N^{1/2}$ segments. We assume that the loops are unentangled because of collapsed conformation as compared to the primary trunk.

(3) The primitive chain is entangled and can move along itself with a curvilinear diffusion coefficient determined from the dynamics of a modified Rouse chain.

(4) The primitive chain has the conformation of a random walk, i.e., the tangents at different points along the trunk are uncorrelated

Second, using the pom-pom model analogy, the diffusion coefficient of a loop point D_l is given by $D_l=(1/2)\times(a^2/\tau_{R\ loop})$, where $\tau_{R\ loop}\sim N$ is the Rouse relaxation time of the loop attached to the loop point. Using the Einstein argument, the drag on a loop point is given by $\zeta_l=k_BT/D_l$. From this we obtain that the friction experienced by the loop point scales as $N\zeta$, where ζ is the friction coefficient of a single Rouse bead in the loop. Thus, the modified Rouse chain, which constitutes the primitive chain, has each of its beads having a friction coefficient of $N\zeta$.

In the above argument we have reduced the structure of the ring polymer to its primary hierarchical level consisting of a primary trunk of $N^{1/2}$ segments having $N^{1/2}$ number of loops attached to it, each consisting of, on an average, $N^{1/2}$ beads. In other words, we have not explicitly invoked the self-similar structure of the lattice tree. In fact we show in Appendix E that such an explicit accounting of the lattice-tree structure, while invoking the Einstein argument and the modified Rouse dynamics consistently at each hierarchical level, indeed gives a friction coefficient of a primary trunk segment scaling as $N\zeta$. The current framework is thus self-consistent. However, in the rest of the work described below we will concern ourselves with only the primary hierarchical level since our main interest is in describing the evolution of the longest length scale and consequently, the slowest dynamics.

The primitive chain and the modified Rouse chain of the PPR framework can be appropriately modeled with a change in static structure. In the case of rings in a melt environment

since $R_g \sim N^{\nu}$, where ν can lie between 1/4 and 1/2 [12,17,18], the characteristic length scale, i.e., the length of the trunk, is expected to be of the order $N^{2\nu}$. We have loops, each containing $N^{1-2\nu}$ segments, attached to these $N^{2\nu}$ trunk segments, acting as frictional constraints to the motion of the trunk. A detailed analysis of the dynamics in the melts based on this physical picture is presented in Sec. V.

In the case of the excluded volume ring since $R_g \sim N^{1/2}$ [12], the length of the trunk is expected to be of order N. The excluded volume ring formulation can be thought of as consisting of N loops, each containing one segment. For this structure we would expect dynamic scalings similar to that of linear chains because the structure is like that of a double-folded ring and the dynamics is expected to be like that of the reptation of a double-folded sausage [15]. Simulations by Cates and Deutsch [12] confirm that the scaling coefficient for swollen rings is similar to that of linear chains.

III. DIFFUSION COEFFICIENT, RELAXATION TIMES, AND DYNAMIC STRUCTURE FACTOR

A. Curvilinear diffusion coefficient

Using the PPR framework one can determine the self-diffusion coefficient, longest relaxation time, and the dynamic structure factor of the ring chain, considering that the dynamics of the trunk of the ring confined in the tube of obstacles governs these aspects. To determine the curvilinear diffusion coefficient of the primitive chain we begin with the dynamics of the modified Rouse chain constituting the primitive chain. We start with the Langevin equation for the nth bead of the chain experiencing an effective friction of $\zeta_{eff}=N\zeta$,

$$\zeta_{eff}\frac{\partial \mathbf{R}_n}{\partial t} = k_{eff}\frac{\partial^2 \mathbf{R}_n}{\partial n^2} + \mathbf{f}_n, \tag{2}$$

where $\mathbf{R}_n$ is the coordinate of the nth bead and $\mathbf{f}_n$ is the stochastic force on the nth bead. Since the loops are considered to contribute only to the friction of the trunk, the potential between beads is not affected by the presence of loops and hence the effective spring constant is given by $k_{eff}=3k_BT/b^2$, however, the effective friction coefficient is given by $\zeta_{eff}=N\zeta$ as argued in the previous section.

From the fluctuation-dissipation theorem we have the moments of the stochastic force ($\mathbf{f}_n$) experienced by the modified Rouse bead given by

$$\langle \mathbf{f}_n(t)\rangle = \mathbf{0},$$

$$\langle [f_{n\alpha}(t) f_{n\beta}(t')]\rangle = 2\zeta_{eff} k_B T \delta(n-m)\delta_{\alpha\beta}\delta(t-t'). \tag{3}$$

We decouple the set of Eq. (2), $n=1,2,\ldots,N^{1/2}$, using the normal coordinate system [see Appendix A, Eqs. (A1)–(A6)] and use Eqs. (3) to determine the different Rouse modes and the relaxation spectrum.

The diffusion coefficient of the center of mass is defined by

$$D_c = \lim_{t\to\infty}\frac{1}{6t}\langle [\mathbf{R}_G(t)-\mathbf{R}_G(0)]^2\rangle. \tag{4}$$

The zeroth normal mode X_0 corresponds to the position of the center of mass of the chain and is given by Eq. (5). The mobility of the center of mass is determined from the corresponding normal mode equation. The diffusion coefficient is given by Eq. (6);

$$\mathbf{R}_G = \frac{1}{N^{1/2}}\int_0^{N^{1/2}} dn \mathbf{R}_n = \mathbf{X}_0, \tag{5}$$

$$D_c = \lim_{t\to\infty}\frac{1}{6t}\sum_{\alpha}\langle [X_{0\alpha}(t)-X_{0\alpha}(0)]^2\rangle. \tag{6}$$

From the normal-mode equations we obtain for ideal rings in the FO environment [using $\nu=1/4$ in Eq. (A5)]

$$\langle [X_{0\alpha}(t)-X_{0\alpha}(0)]^2\rangle = 2\frac{k_BT}{N^{1/2}\zeta_{eff}}\delta_{\alpha\alpha}t. \tag{7}$$

Substituting Eq. (7) in Eq. (6) we obtain

$$D_c = \frac{k_BT}{N^{1/2}\zeta_{eff}}. \tag{8}$$

Using $\zeta_{eff}=N\zeta$ we have

$$D_c = \frac{k_BT}{N^{3/2}\zeta}. \tag{9}$$

The scaling arguments of Obukhov *et al.* [13] have $N^{1/2}$ kinks diffusing over a linear dimension a to give the center-of-mass curvilinear diffusion coefficient scaling as $N^{1/2}(a/N)^2 \sim N^{-3/2}$, a scaling satisfied by Eq. (9).

B. Self-diffusion coefficient and relaxation times

The higher-order Rouse modes can be determined from the decoupled normal-mode equations [see the Appendix B, Eq. (B1)], $p=1,2,\ldots,\infty$. The modified Rouse relaxation spectrum for the chain is given by

$$\tau_p = \frac{1}{3}\frac{1}{p^2}\frac{b^2}{\pi^2}\frac{\zeta}{k_BT}N^2. \tag{10}$$

We now consider the case where the primitive chain of length $L_{trunk}=N^{1/2}b^2/a$ is confined in a tube formed by the FO environment and relaxes by reptation dynamics similar to that of a linear chain. The reptation of the trunk is governed by the reptation equation given by

$$\frac{\partial}{\partial t}\phi(s,s';t) = D_c\frac{\partial^2}{\partial s^2}\phi(s,s';t), \tag{11}$$

where we have $\phi(s,s';t)=\langle [\mathbf{R}(s,t)-\mathbf{R}(s',0)]^2\rangle$ and $\mathbf{R}(s,t)$ is the position vector of a bead at a curvilinear distance s at time t. The associated initial and boundary conditions for this equation are given by

$$\phi(s,s';0) = a|s-s'|, \tag{12}$$

$$\left.\frac{\partial}{\partial s}\phi(s,s';t)\right|_{s=L_{trunk}} = a, \tag{13}$$

$$\left.\frac{\partial}{\partial s}\phi(s,s';t)\right|_{s=0} = -a. \tag{14}$$

The diffusion coefficient calculated from the modified Rouse chain becomes the curvilinear diffusion coefficient of the primitive chain in the tube formulation. We use the curvilinear diffusion coefficient of the primitive chain given by Eq. (9) to determine the self-diffusion coefficient and the longest relaxation time of the ring polymer for ideal rings in the FO environment as (see Appendix C use $\nu=1/4$)

$$D = \frac{1}{3}\frac{k_B T}{N^2 \zeta}\frac{a^2}{b^2}, \tag{15}$$

$$\tau_d = \frac{1}{\pi^2}\frac{b^4}{a^2}\frac{\zeta}{k_B T}N^{5/2}. \tag{16}$$

The exponents determining the dependence on the molecular weight (N) in the theoretical predictions of Eqs. (15) and (16) agree with the scaling exponents of Obukhov *et al.* [13] for the self-diffusion coefficient and the longest relaxation time.

C. Dynamic structure factor

The dynamic structure factor $g(\mathbf{k},t)$ corresponding to the primitive chain can also be determined from the reptation picture in a fashion similar to that of the linear chain. In this case one has to consider that the evolution of the structure factor corresponds to the evolution of the hypothetical trunk of the ring polymer,

$$g(\mathbf{k},t) = \frac{N^{1/2}}{L_{trunk}^2}\int_0^{L_{trunk}} ds \int_0^{L_{trunk}} ds' \langle \exp\{i\mathbf{k}\cdot[\mathbf{R}(s,t) - \mathbf{R}(s',0)]\}\rangle. \tag{17}$$

Based on the reptation formulation we obtain $g(\mathbf{k},t)$ as

$$g(\mathbf{k},t) = \sum_{p=1}^{\infty} \frac{2\mu N^{1/2}}{\alpha_p^2(\mu^2+\alpha_p^2+\mu)} \sin^2\alpha_p \times \exp\left(-4\frac{D_c t \alpha_p^2}{L_{trunk}^2}\right), \tag{18}$$

where

$$\mu = \frac{\mathbf{k}^2}{12} L_{trunk} a. \tag{19}$$

α_p are the positive solutions of the equation

$$\alpha_p \tan\alpha_p = \mu. \tag{20}$$

There are two limits at which the dynamic structure factor can be obtained. For $\mu << 1$ we focus on a length scale larger than the size of the polymer chain and $g(\mathbf{k},t)$ is given by

$$g(\mathbf{k},t) = N^{1/2}\exp(-D\mathbf{k}^2 t). \tag{21}$$

For $\mu >> 1$ we focus on a smaller length scale than the size of the polymer chain and $g(\mathbf{k},t)$ is given by

$$g(\mathbf{k},t) = \frac{12}{\mathbf{k}^2 b^2}\Psi(t), \tag{22}$$

where $\Psi(t)$ is the fraction of chain in the original tube at time t. Since we are concerned in this work with only the motion of the longest length scale, i.e., the entangled primary trunk, Eq. (22) above is applicable for wave vectors in the range $N^{-1/4} << k << N^{-1/8}$.

IV. RELAXATION MODULUS

Typically in experiments we explore two regimes of system behavior, viz., the high-frequency regime to explore the response of parts of the chain and the low-frequency regime to explore the entire chain response to an applied deformation gradient. Below the obstacle linear dimension a, the trunk chain does not see the constraints and sections of the chain relax by three-dimensional (3D) Rouse modes. The time scale of relaxation associated with this length scale a is the same as the time taken for a monomer to have an average mean-square displacement of a^2. In our system we use the modified Rouse formulation to calculate monomer displacement along the trunk since we know that beads along the trunk experience a friction $N\zeta$. Based on this formulation we have the time taken for such a displacement of monomer along the trunk given by (see the Appendix D Eq. (6); use $\nu=1/4$)

$$\tau_e = \frac{a^4}{b^2}\frac{\pi}{12}\frac{N\zeta}{k_B T}. \tag{23}$$

For times $t > \tau_e$ the chain starts encountering obstacles. The dynamics is no longer modified Rouse dynamics beyond this time scale.

The relaxation modulus has to be obtained in two steps because of the distinct dynamics scenario at different length scales. For time scale $t < \tau_e$ the relaxation modulus is obtained from the modified Rouse dynamics picture and for $t > \tau_e$ the reptation picture is invoked. For obtaining the relaxation modulus we first start with the microscopic expression for the stress tensor given by

$$\sigma_{\alpha\beta} = \frac{c_t}{N^{1/2}} k_{eff} \int_0^{N^{1/2}} dn \left\langle \frac{\partial R_{n\alpha}}{\partial n}\frac{\partial R_{n\beta}}{\partial n}\right\rangle. \tag{24}$$

Since all the stress in the system is stored by the orientation of the trunk segments rather than the entire polymer, we use the concentration of segments along trunk c_t of the chain rather than the concentration of segments on the entire polymer c in the stress-tensor expression.

For the case $t < \tau_e$, we may use normal coordinates to simplify Eq. (24) and obtain

$$\sigma_{\alpha\beta} = 2\frac{c_t}{N}k_{eff}\pi^2\sum_{p=1}^{\infty} p^2\langle X_{p\alpha}X_{p\beta}\rangle. \tag{25}$$

We now impose a homogeneous deformation gradient $\bar{v}(\mathbf{r},t)=\bar{\bar{\kappa}}(t)\cdot\mathbf{r}$ on the FO environment. During such a deformation the Langevin equation for the pth normal coordinate $\mathbf{X}_p$ becomes

$$\frac{\partial \mathbf{X}_p}{\partial t} = -\frac{k_p}{\zeta_p}\mathbf{X}_p + \frac{1}{\zeta_p}\mathbf{f}_p + \bar{\bar{\kappa}}(t)\cdot\mathbf{X}_p. \tag{26}$$

From the Langevin equation (26) we obtain the equation for the correlation $\langle X_{p\alpha}X_{p\beta}\rangle$ as

$$\frac{\partial\langle X_{p\alpha}X_{p\beta}\rangle}{\partial t} = -2\frac{k_p}{\zeta_p}\langle X_{p\alpha}X_{p\beta}\rangle + \frac{1}{N^{3/2}\zeta}k_BT\delta_{\alpha\beta} + \kappa_{\alpha\mu}\langle X_{p\mu}X_{p\beta}\rangle + \kappa_{\beta\mu}\langle X_{p\alpha}X_{p\mu}\rangle. \tag{27}$$

Equation (27) can be solved to obtain $\langle X_{p\alpha}X_{p\beta}\rangle$ for any given homogeneous deformation gradient. For homogeneous shear where $\bar{\bar{\kappa}}(t)$ is given by

$$\begin{bmatrix} 0 & \kappa(t) & 0 \\ 0 & 0 & 0 \\ 0 & 0 & 0 \end{bmatrix},$$

we have the equation for the xy component of the correlation given by

$$\frac{\partial\langle X_{px}X_{py}\rangle}{\partial t} = -2\frac{k_p}{\zeta_p}\langle X_{px}X_{py}\rangle + \kappa(t)\langle X_{py}^2\rangle. \tag{28}$$

Considering the system to be close to equilibrium we have $\langle X_{py}^2\rangle = k_BT/k_p$, which using the solution to Eq. (28) is obtained as

$$\langle X_{px}X_{py}\rangle = \frac{k_BT}{k_p}\int_{-\infty}^{t} dt_1 \exp\left(\frac{-2(t-t_1)}{\tau_p}\right)\kappa(t_1). \tag{29}$$

Substituting Eq. (29) in Eq. (25) we obtain

$$\sigma_{xy} = 2\frac{c_t}{N}k_{eff}\pi^2\sum_{p=1}^{\infty} p^2\frac{k_BT}{k_p}\times\int_{-\infty}^{t} dt_1 \exp\left(\frac{-2(t-t_1)}{\tau_p}\right)\kappa(t_1). \tag{30}$$

The phenomenological expression for the stress tensor in terms of the relaxation modulus is given by

$$\sigma_{xy}(t) = \int_{-\infty}^{t} dt_1 G(t-t_1)\kappa(t_1). \tag{31}$$

Comparing Eq. (30) with Eq. (31) we obtain

$$G(t) = \frac{c_t}{N^{1/2}}k_BT\sum_{p=1}^{\infty}\exp\left(-2\frac{t}{\tau_p}\right). \tag{32}$$

For the case $t > \tau_e$ the reptation framework is invoked wherein the stress memory in the system at any time corresponds to the fraction of the chain in the original tube at that time. From the reptation equation the fraction of chain in a given tube, $\Psi(t)$, and the associated relaxation modulus, $G(t)$ are given by

$$\Psi(t) = \frac{8}{\pi^2}\sum_{p=1,odd}^{\infty}\frac{1}{p^2}\exp\left(\frac{-tp^2}{\tau_d}\right), \tag{33}$$

$$G(t) = G_0\Psi(t). \tag{34}$$

At time $t=\tau_e$ we have from the modified Rouse dynamics $G(\tau_e)=(c_t/\sqrt{2}\pi)k_BT(b^2/a^2)$ and from the reptation dynamics $G(\tau_e)=G_0\Psi(\tau_e)$. For large N we can see from Eqs. (16) and (23) that the time scale $\tau_e << \tau_d$, which makes it reasonable to assume that $\Psi(\tau_e)=1$. By the comparison of $G(\tau_e)$ from Rouse dynamics and reptation we determine the value of the constant G_0 as given in Eq. (35). Then the expression for the relaxation modulus for time $t \geqq \tau_e$ is given by Eq. (36).

$$G_0 = \frac{c_t}{\sqrt{2}\pi}k_BT\frac{b^2}{a^2}, \tag{35}$$

$$G(t) = \frac{4\sqrt{2}}{\pi^3}c_tk_BT\frac{b^2}{a^2}\sum_{p=1,odd}^{\infty}\frac{1}{p^2}\exp\left(\frac{-tp^2}{\tau_d}\right). \tag{36}$$

V. MELT OF RINGS

The analysis for the FO environment can be extended to the melt of rings by retaining one assumption and incorporating two modifications. The assumption we make is that the static structure of a ring in its melt can be described as consisting of a longest characteristic length scale (the primitive chain) having fast relaxing friction-contributing loops attached to it. Of the two modifications, the first modification corresponds to the static structure; based on scaling arguments and computer simulations [12,17,18] the size of the ring chain in melt R_g is determined to be of the order $\sim N^{\nu}$, where ν can lie between the extremes of 1/4 and 1/2. Thus the primitive chain would scale as $N^{2\nu}$. The collapsed structure of rings in the melt environment causes the entanglement molecular weight or the entanglement spacing of the ring polymeric system to be different from that of linear chains. The entanglement molecular weight is an experimentally obtained parameter in the tube model. It is obtained from the plateau modulus, G_N^0 data, and for linear polymers can be calculated using the expression of form [19]

$$M_e = \frac{1}{\sqrt{2}\pi}\frac{\rho N_Ak_BT}{G_N^0}. \tag{37}$$

From the entanglement molecular weight the average number of Kuhn segments present between entanglements N_e can be calculated.

Since the ring polymer takes a more collapsed conformation than the linear in a melt environment, two possible scenarios for estimating N_e can be considered. In the first scenario we may expect that the number of segments between entanglements for a given entanglement spacing a is more for rings. We propose the following way to obtain the

number of segments between entanglements for rings N_e^r. In the case of linear chains we have $a^2/b^2=N_e^l$ based on the random-walk structure and in the case of rings we have $a^2/b^2=(N_e^r)^{2\nu}$ based on the self-similar structure of the lattice animal. Equating the right-hand side of the expressions for a^2/b^2 we have $N_e^r=(N_e^l)^{2\nu}$. It can be seen from this expression for N_e^r that the collapsed conformation of rings causes the number of segments between a given entanglement spacing to be greater than that for linear chains.

The second scenario could be that we hold the molecular weight between entanglements for rings to be the same as for linear chains, whereas the entanglement spacing a changes due to the difference in the static conformation of the rings. Due to the collapsed conformation of the rings, the entanglement spacing is expected to be smaller for rings as compared to linear chains. Based on this picture we have the entanglement spacing for rings given by $a_r=(N_e)^{\nu}b$, which is smaller than the entanglement spacing for linear chains $a_l=N_e^{1/2}b$.

Several simulations on the melt of rings [17,23,24] seem to indicate that while high molecular-weight linear polymers can feel the effects of entanglements in their melt state, rings of the same molecular weight (and identical chemical structure) are not effectively entangled. Experimental evidence indicates that the rings are less effectively entangled as compared to linear chains. Roovers [9], using dynamic oscillatory data, and McKenna *et al.* [20], using creep data, showed that the plateau modulus of ring melts was approximately half that for the linears of similar molecular weight. Later Roovers [7] also claimed that the (much diffused) plateau modulus for a highly pure polybutadiene ring polymer melt was as low as one-fifth that of the linears of similar molecular weight. Thus rings do seem to entangle in a melt state, however, they do so only at much higher molecular weights compared to their linear counterparts. Further support comes from recent simulations of Muller *et al.* [18] who show that for semiflexible rings and high molecular-weight flexible rings a significant fraction of the total monomer density is contributed by the neighbors of a given ring molecule, which indicates that such ring molecules could be well entangled.

In scenario one discussed above we have already shown that the number of segments between entanglements and hence the entanglement molecular weight is larger for rings based on the static structure. As a result the number of entanglements for a given molecular weight would indeed be less for rings as compared to linear chains. However, there is one more reason for why the plateau modulus of the melt of rings could be lower than that for a linear chain melt. In rings the orientation of the trunk governs the long-term dynamics and hence the effective entanglement of the trunk is the point of concern. The density ρ in Eq. (37) for the ring chain no longer corresponds to the bulk density of the polymer but rather to the density of trunks in the system. This density is lower as compared to that of the bulk density due to the presence of a large number of loops in the system. The dilution effect is also partly responsible for the reduction of the plateau modulus.

If we consider c_t the concentration of the number of segments lying along the trunk of the ring, then the number of trunks per unit volume in the melt is $c_t/N^{2\nu}$ since the trunk contains $N^{2\nu}$ segments. The number of rings per unit volume is given by the concentration of the number of segments per unit volume divided by the number of segments per ring, c/N. Considering that the number of trunks should be the same as the number of rings, we equate the number of trunks and the number of ring chains,

$$\frac{c_t}{N^{2\nu}}=\frac{c}{N}, \quad c_t=\frac{c}{N^{1-2\nu}}. \tag{38}$$

Substituting for c_t in Eq. (36) we obtain

$$G(t)=\frac{4\sqrt{2}}{\pi^3}\frac{c}{N^{1-2\nu}}k_BT\frac{b^2}{a^2}\sum_{p=1,odd}^{\infty}\frac{1}{p^2}\exp\left(\frac{-tp^2}{\tau_d}\right). \tag{39}$$

It is clear from the above expression that the density is diluted by a factor of $1/N^{1-2\nu}$ when we consider only the density of segments along the trunk of the ring chain. Thus we expect the plateau modulus of the ring melt to be smaller than the plateau modulus of the linear melt by a factor of $1/N^{1-2\nu}$.

Further, zero shear viscosity (ZSV) measurements on polybutadiene rings of MW 6.0×10^4 g/mol indicate that the ZSV of ring melt is approximately ten times lower than that of the corresponding linear melt [7]. This can be understood in terms of the ZSV scaling comparisons of linear chains and rings. The ratio of the ZSV of the ring to that of the linear chain is given by

$$\frac{\eta_{0r}}{\eta_{0l}}=\frac{G_{Nr}^0}{G_{Nl}^0}\frac{\tau_{dr}}{\tau_{dl}}. \tag{40}$$

For the melt of rings we have $\tau_{dr}\sim N^{2(1+\nu)}$ [see Eq. (C1)], while for linear chains we have $\tau_{dl}\sim N^3$. Thus for large N, given $\nu<1/2$, we have $\tau_{dr}\ll\tau_{dl}$. From Eq. (40) we calculate the ZSV ratio between the melt of the ring and the melt of linear scales as $N^{-2(1-2\nu)}$.

The ring-to-linear ratio of the plateau modulus, relaxation time, and ZSV can be calculated based on both the pictures of changed entanglement molecular weight $N_e^r=(N_e^l)^{1/2\nu}$ and changed entanglement spacing $a_r=N_e^{-(1-2\nu)/2}a_l$ for rings. Based on the former picture we obtain

$$\frac{G_{Nr}^0}{G_{Nl}^0}=\frac{c_t}{c}=\frac{1}{N^{1-2\nu}}, \tag{41}$$

$$\frac{\tau_{dr}}{\tau_{dl}}=\frac{1}{N^{1-2\nu}}, \tag{42}$$

$$\frac{\eta_{0r}}{\eta_{0l}}=\frac{1}{N^{2(1-2\nu)}}. \tag{43}$$

Based on the latter picture we obtain

$$\frac{G_{Nr}^0}{G_{Nl}^0}=\frac{c_t}{c}N_e^{1-2\nu}=\left(\frac{N_e}{N}\right)^{1-2\nu}, \tag{44}$$

$$\frac{\tau_{dr}}{\tau_{dl}}=\left(\frac{N_e}{N}\right)^{1-2\nu}, \tag{45}$$

$$\frac{\eta_{0r}}{\eta_{0l}} = \left(\frac{N_e}{N}\right)^{2(1-2\nu)}. \quad (46)$$

We compare the results based on the above pictures with the experimental results of Roovers [7](see Table III) for the lower limits $\nu=1/4$, $\nu=3/10$, and the conjecture value $\nu=2/5$ proposed by Cates and Deutsch [12].

Further, we obtain the ratio τ_1/τ_e, a measure of how fast a crossover occurs from Rouse to reptation regime with N/N_e, as follows:

$$\frac{\tau_1}{\tau_e} = \frac{4}{\pi^3}\frac{b^4}{a^4}N^{4\nu} = \frac{4}{\pi^3}\left(\frac{N}{N_e^r}\right)^{4\nu}. \quad (47)$$

It can be seen from the expression that τ_1/τ_e scales weakly as $(N/N_e^r)^{4\nu}$ for $\nu<1/2$ in comparison to a stronger scaling of $(N/N_e^l)^2$ for linear chains. Thus, the crossover to reptation happens for relatively lower values of N in the case of linear chains as compared to rings, a result that is in agreement with the simulation of Müller *et al.* [17].

We find that the theoretical predictions of the plateau modulus, relaxation times, and ZSV by the PPR framework vary sharply with exponent ν (Table III). Since there is some uncertainty regarding the exact value of ν for a melt of rings, we have attempted to compare the PPR predictions of linear viscoelastic variables with experimental data for various values of ν. In particular, we have chosen the rheological data of Roovers [7] on polybutadiene (PBD) polymers. We specifically looked at the data of two samples: a linear PBD (sample KPBD34PC, MW$=5.7\times10^4$ g/mol, $\eta_0=6.7\times10^5 P$) and a ring PBD (sample KPBD34B3, MW$=6.0\times10^4$ g/mol, $\eta_0=6.3\times10^4 P$). The ring sample was free of linear contaminants that could potentially have substantially altered the rheology of the ring melts [7]. The linear and the ring PBDs have similar molecular weight and polydispersity, however, the ZSV and the plateau modulus of the ring sample were lower than those for the linear sample [7].

In order to compare PPR theory predictions with experimental data we need parameters concerning chain dimensions and entanglement spacing for PBD. The molecular parameters $a\approx45$ Å, $b\approx11$ Å, $N_e^l\approx15.5$ were obtained from Fetters *et al.* [21] for the PBD-62 sample (see also Table II of Ref. [22]). This linear PBD contains 62% 1,2 microstructure, which is similar to the 63% 1,2 microstructure in Roovers' PBD sample. We obtained the concentration (c) of Kuhn segments per unit volume in the melt of linear chains by using the value of the plateau modulus ($G_N^0=0.81$ MPa) tabulated for PBD-62 in the expression $G_N^0=[1/(\sqrt{2}\pi)]ck_BT(b^2/a^2)$. In addition to parameters concerning chain dimension and entanglement spacing, we need a friction coefficient of a single Rouse bead (ζ). This was obtained by fitting the predictions of DE theory to the experimental data of Roovers' linear sample KPBD34PC (see Fig. 4). The same friction coefficient was used for ring PBD.

We find that the predictions of the ZSV ratios are in close agreement with the experimental data for $\nu=3/10$ for the modified entanglement spacing scenario and $\nu=2/5$ for the modified entanglement molecular-weight scenario. The experimental ring-linear ratios of the plateau modulus and the longest relaxation times (taken as the inverse of the crossover frequency in the experimental data) do not compare very well with the PPR model predictions. Figures 4 and 5 show the comparison between the experimental frequency data and the PPR predictions for the two scenarios, modified entanglement molecular weight ($\nu=2/5$) and modified entanglement spacing ($\nu=3/10$), respectively. The predictions of the PPR model in the linear viscoelastic regime are encouragingly close to the experimental data for both cases. Thus the PPR model by itself does not clarify as to which of the two scenarios (and consequently what value of ν) should be adopted for understanding the dynamics of rings.

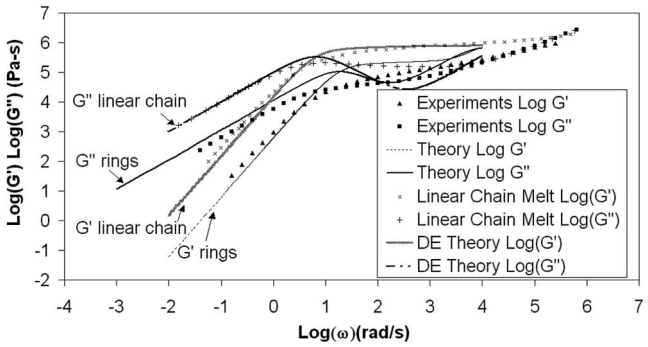

FIG. 4. Comparison between Roovers experimental data for the ring sample KPBD34B3 and PPR theory with exponent $\nu=0.4$ in the modified entanglement molecular-weight scenario.

We expect the theory to overpredict the relaxation time and viscosity since we have not considered contour length fluctuation (CLF) for the trunk. CLF reduces the disengagement time (longest relaxation time) for the trunk from its tube of confinement and hence reduces the viscosity. In the case of a ring in the melt the longest relaxation-time scaling, without CLF, is given by $\sim\bar{L}_{trunk}^2/D_c$, where $\bar{L}_{trunk}=N^{2\nu}b^2/a$ is the average contour length. This yields $\tau_d\sim N^{2(1+\nu)}b^4/a^2$ for the ring without CLF. The relaxation time is reduced by CLF corrections and is given by

$$\tau_d^{CLF} \simeq \frac{(\bar{L}_{trunk}-\Delta\bar{L}_{trunk})^2}{D_c},$$

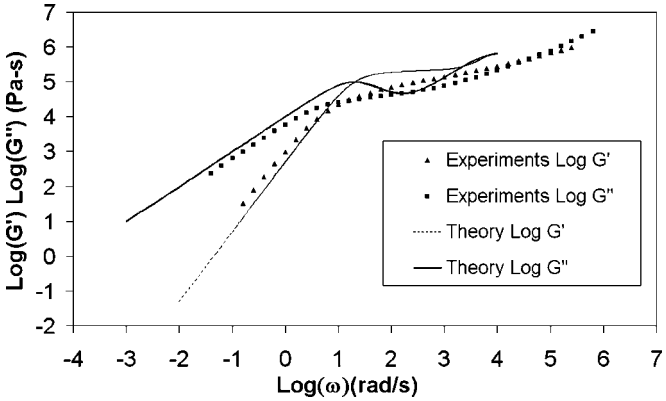

FIG. 5. Comparison between Roovers experimental data for the ring sample KPBD34B3 and PPR theory with exponent $\nu=0.3$ in the modified entanglement spacing scenario.

TABLE I. Comparison between the scaling results and the expressions derived using the PPR framework.

Quantity	Scaling[a]	PPR
Curvilinear diffusion coefficient	$\sim N^{-3/2}$	$D_c=\frac{k_BT}{\zeta}N^{-3/2}$
Self-diffusion coefficient	$\sim N^{-2}$	$D=\frac{1}{3}\frac{k_BT}{\zeta}\frac{a^2}{b^2}N^{-2}$
Longest relaxation time	$\sim N^{5/2}$	$\tau_d=\frac{1}{\pi^2}\frac{b^4}{a^2}\frac{\zeta}{k_BT}N^{5/2}$

[a]Reference [13].

$$\tau_d^{CLF} \simeq \left(\frac{N^{2(1+\nu)}b^4}{a^2} - \frac{2}{\sqrt{3}}\frac{N^{\nu+2}b^3}{a} + \frac{N^2b^2}{3}\right)\frac{\zeta}{k_BT}, \quad (48)$$

where $\Delta\bar{L}_{trunk}=(N^{2\nu}b^2/3)^{1/2}$ is the average fluctuation.

In Eqs. (48) the first term corresponds to the scaling without CLF corrections. The second and third terms correspond to corrections effected by CLF. It can be seen that CLF-induced corrections are significant for finite N and the higher the value of N the less significant are the corrections. Further, CLF-introduced corrections are expected to be considerable in the case of a more collapsed ring when the trunk has longer loops associated with it. For example, consider the comparison between the cases of $\nu=2/5$ and $\nu=1/4$. We have

$$\tau_d^{CLF} \simeq \left(\frac{N^{14/5}b^4}{a^2} - \frac{2}{\sqrt{3}}\frac{N^{12/5}b^3}{a} + \frac{N^2b^2}{3}\right)\frac{\zeta}{k_BT},$$

$$\tau_d^{CLF} \simeq \left(\frac{N^{5/2}b^4}{a^2} - \frac{2}{\sqrt{3}}\frac{N^{9/4}b^3}{a} + \frac{N^2b^2}{3}\right)\frac{\zeta}{k_BT}. \quad (49)$$

As the ring becomes more collapsed it can be seen that the exponent of N in the second term (correction term) approaches the exponent in the first term.

VI. CONCLUSION

In this paper we have developed the PPR framework for studying the dynamics of flexible ring polymers in fixed and moving obstacle environments. The PPR approach is inspired by the pom-pom model for branched polymers and is based on the tube framework. In developing this framework we have exploited the correspondence between the static structure of an ideal ring polymer in the FO environment and an ideal randomly branched polymer. The framework was used to derive analytical expressions for the curvilinear diffusion coefficient, self-diffusion coefficient, longest relaxation time, and dynamic structure factor. The derived expressions are in good agreement with the scaling theories (see Table I).

The framework is general in the sense that as long as the static structure of the ring can be described in terms of a longest characteristic length scale, viz., the primary trunk, and collapsed loops attached to it, appropriate modifications can be incorporated into the framework in terms of the size of the trunk and the loops. The longer the trunk, the larger would be the number of loops associated with it, but the smaller would be the size of the loops. In general, our interest in this paper was restricted to studying the dynamics of the longest length scale of the ring structure. The primary trunk was modeled as a modified Rouse chain for which the fast relaxing loops associated with it contribute only to the friction of the trunk. The modified Rouse chain bead friction can be modified to incorporate the extra friction contributed by the loops based on the pom-pom picture using Rouse dynamics for the relaxation of loops instead of arm retraction.

TABLE II. General scaling results for a ring with its $R_g \sim N^{\nu}$.

Quantity	Scaling from PPR
Number of trunk segments	$N^{2\nu}$
Number of loop segments	$N^{1-2\nu}$
Rouse bead friction/τ_e	$N^{2(1-2\nu)}$
Curvilinear diffusion coefficient	$N^{-2(1-\nu)}$
Self-diffusion coefficient	N^{-2}
Longest relaxation time	$N^{2(1+\nu)}$
Plateau modulus	$N^{2\nu-1}$
Viscosity	$N^{4\nu+1}$

The scaling relations of the dynamic quantities would appropriately change with the change in the static structure (Table II). It may be of some interest to note that for an unentangled ring in its melt, for which the scaling exponent of the radius of gyration with molecular weight is close to 0.4, the diffusion coefficient derived from the modified Rouse dynamics scales as $D\sim N^{-1.2}$ (see Table II) and the Rouse relaxation time scales as $\sim N^2$. This appears to be in agreement with recent simulation studies on unentangled rings in melt [18,23]. Note that for a swollen ring chain for which $R_g \sim N^{1/2}$, we recover the linearlike scaling for the various parameters in Table II.

Further, we have also explored the linear viscoelastic response of high molecular-weight entangled rings and derived the relaxation modulus in the linear regime. We have assumed in the entire analysis that the relaxation of the loop is essential for the mobility of the trunk of the ring. In this the predominant length scale, viz., the trunk relaxes much more slowly than the loops sitting on it. This is true even when the number of segments composing the loops and trunk are the same since the loop static structure is much more collapsed than that of the trunk.

The extension of the results to melts is not straightforward as it involves a couple of subtle issues that need to be addressed. The first of these issues is the modification of entanglement molecular weight or the entanglement spacing for the melt of rings. The second issue relates to accounting for the dilution effects of the relaxed loop segments. A comparison of theoretically calculated ratios of the ring-to-linear plateau modulus, relaxation times, and ZSV with experimental results of Roovers [7] for the melt of pure polybutadiene

TABLE III. Comparison between the PPR framework results and the experimental results for the PBD ring of MW 6.0×10^4 g/mol and $M_e = 2750$ g/mol ($N \approx 341$, $N/N_e \approx 22$).

Quantity[a]	Experiments[b]	PPR $N_e^r = (N_e^l)^{1/2\nu}$	PPR $a_r = a_l N_e^{-(1-2\nu)/2}$
Ratio of plateau modulus $\left(\frac{G_{Nr}^0}{G_{Nl}^0}\right)$	0.15	($\nu = 1/4$) 0.054	($\nu = 1/4$) 0.21
Ratio of relaxation times $\left(\frac{\tau_{dr}}{\tau_{dl}}\right)$	0.63	0.054	0.21
Ratio of ZSV $\left(\frac{\eta_{0r}}{\eta_{0l}}\right)$	0.094	0.003	0.046
Ratio of plateau modulus $\left(\frac{G_{Nr}^0}{G_{Nl}^0}\right)$	0.15	($\nu = 3/10$) 0.097	($\nu = 3/10$) 0.29
Ratio of relaxation times $\left(\frac{\tau_{dr}}{\tau_{dl}}\right)$	0.63	0.097	0.29
Ratio of ZSV $\left(\frac{\eta_{0r}}{\eta_{0l}}\right)$	0.094	0.009	0.084
Ratio of plateau modulus $\left(\frac{G_{Nr}^0}{G_{Nl}^0}\right)$	0.15	($\nu = 2/5$) 0.31	($\nu = 2/5$) 0.54
Ratio of relaxation times $\left(\frac{\tau_{dr}}{\tau_{dl}}\right)$	0.63	0.31	0.54
Ratio of ZSV $\left(\frac{\eta_{0r}}{\eta_{0l}}\right)$	0.094	0.096	0.29

[a] r denotes ring and l denotes linear.
[b] The linear chains MW is 5.710^4 while the ring MW is 6.010^4.

rings of MW 6.0×10^4 g/mol having a M_e of 2750 g/mol [7] is presented in Table III.

We have compared our predictions with only one experimental rheological data set of Roovers [7] that is believed to be obtained for a melt of pure rings having no linear contaminants that could otherwise dramatically affect the rheological behavior. The comparison indicates that depending on the scenario adapted, modified entanglement molecular weight or entanglement spacing, the PPR framework gives reasonable predictions of the ZSV ratio and frequency sweep experimental data but for different values of the static scaling exponent ν. The Cates and Deutsch conjecture of $\nu = 2/5$ [12] and the results of early simulations by Müller *et al.* [17] go well with the modified entanglement molecular-weight scenario. In a more recent work of Müller *et al.* [18] it is argued that the use of a general exponent ν lying between 1/4 and 1/2 is more appropriate. Such a general exponent ν will go well with both the scenarios. It is thus not clear as to which of the two scenarios is to be coupled with the PPR framework for predicting the experimental results.

ACKNOWLEDGMENTS

B.I. would like to acknowledge financial assistance from the Council of Scientific and Industrial Research. The authors wish to thank Professor Roovers for making available his experimental data for use in the manuscript. The authors also wish to acknowledge the valuable suggestion of Dr. V. Shankar (IIT Kanpur) that helped us improve the analysis.

APPENDIX A: NORMAL COORDINATES

Normal coordinates are defined by

$$\mathbf{R}_n = \mathbf{X}_0 + 2\sum_{p=1}^{\infty} \mathbf{X}_p \cos\left(\frac{p\pi n}{N^{2\nu}}\right), \tag{A1}$$

$$\mathbf{f}_n = \frac{\mathbf{f}_0}{N^{2\nu}} + \frac{1}{N^{2\nu}}\sum_{p=1}^{\infty} \mathbf{f}_p \cos\left(\frac{p\pi n}{N^{2\nu}}\right), \tag{A2}$$

$$\mathbf{X}_p = \frac{1}{N^{2\nu}}\int_0^{N^{2\nu}} dn \cos\left(\frac{p\pi n}{N^{2\nu}}\right)\mathbf{R}_n, \tag{A3}$$

$$\mathbf{f}_p = 2\int_0^{N^{2\nu}} dn \cos\left(\frac{p\pi n}{N^{2\nu}}\right)\mathbf{f}_n. \tag{A4}$$

In the above equations ν is defined as the scaling exponent in $R_g \sim N^{\nu}$. Thus, for an ideal ring in the FO environment $\nu = 1/4$ and for a melt of the rings ν can lie between 1/4 and 1/2.

The transformation of Eq. (2) using normal coordinates decouples the set of equations. By equating the coefficients of $\cos(p\pi n/N^{2\nu})$ we obtain

$$\zeta_{eff}\frac{\partial \mathbf{X}_0}{\partial t} = \frac{\mathbf{f}_0}{N^{2\nu}}, \tag{A5}$$

$$2\zeta_{eff}\frac{\partial \mathbf{X}_p}{\partial t} = -2k_{eff}\frac{p^2\pi^2}{N^{4\nu}}\mathbf{X}_p + \frac{\mathbf{f}_p}{N^{2\nu}}. \tag{A6}$$

APPENDIX B: HIGHER ROUSE MODES

The decoupled equations for the higher normal modes are given by

$$\zeta_p \frac{\partial \mathbf{X}_p}{\partial t} = -k_p \mathbf{X}_p + \mathbf{f}_p, \tag{B1}$$

where

$$\zeta_p = 2N^{2\nu}\zeta_{eff}, \quad k_p = 2k_{eff}\frac{p^2\pi^2}{N^{2\nu}}. \tag{B2}$$

The solution to Eq. (B1) is given by

$$\mathbf{X}_p(t) = \frac{1}{\zeta_p}\int_{-\infty}^{t} dt_1 \exp\left(\frac{-(t-t_1)}{\tau_p}\right)\mathbf{f}_p(t_1), \tag{B3}$$

where $\tau_p = \zeta_p/k_p$.

Substituting for ζ_p and k_p from Eq. (B2) and using $\zeta_{eff} = N^{2(1-2\nu)}\zeta$ and $k_{eff} = 3k_BT/b^2$, we have

$$\tau_p = \frac{1}{p^2}\frac{1}{3}\frac{b^2}{\pi^2}\frac{\zeta}{k_BT}N^2. \tag{B4}$$

From this we see that the longest relaxation time for Rouse type relaxation of the trunk is

$$\tau_1 = \frac{1}{3}\frac{b^2}{\pi^2}\frac{\zeta}{k_BT}N^2. \tag{B5}$$

The correlation function $\langle X_{p\alpha}(t)X_{q\beta}(0)\rangle$ is of considerable importance in determining the stress in the system. In order to determine it we first obtain from Eq. (B3)

$$\langle X_{p\alpha}(t)X_{q\beta}(0)\rangle = \frac{1}{\zeta_p^2}\int_{-\infty}^{t} dt_1 \int_{-\infty}^{0} dt_2 \exp\left(\frac{-(t-t_1)}{\tau_p}\right) \times \exp\left(\frac{t_2}{\tau_q}\right)\langle f_{p\alpha}(t_1)f_{q\beta}(t_2)\rangle. \tag{B6}$$

Using the fluctuation-dissipation theorem given by Eq. (3) and the normal coordinates transformation we obtain

$$\langle [f_{p\alpha}(t_1)f_{q\beta}(t_2)]\rangle = 2\zeta_p k_BT\delta_{pq}\delta_{\alpha\beta}\delta(t_1-t_2). \tag{B7}$$

Using Eq. (B7) in Eq. (B6), we obtain

$$\langle (X_{p\alpha}(t)X_{q\beta}(0)\ \rangle = \frac{k_BT}{k_p}\delta_{pq}\delta_{\alpha\beta}\exp\left(\frac{-t}{\tau_p}\right). \tag{B8}$$

APPENDIX C: REPTATION

The solution for Eq. (11) with the initial and boundary conditions, Eqs. (12)–(14) is given by

$$\phi(s,s';t) = a|s-s'| + 2D_c\frac{a}{L}t + 4\frac{La}{\pi^2}\sum_{p=1}^{\infty}\frac{1}{p^2}\left[1-\exp\left(-\frac{tp^2}{\tau_d}\right)\right] \times \cos\left(\frac{p\pi s}{L}\right)\cos\left(\frac{p\pi s'}{L}\right), \tag{C1}$$

where $\tau_d = 1/(\pi^2)(b^4/a^2)(\zeta/k_BT)N^{2(1+\nu)}$.

In the lim $s' \to s$ we have $\phi(s;t) = \langle [\mathbf{R}(s,t)-\mathbf{R}(s,0)]^2\rangle$, the mean-square displacement of the bead on the sth position along the chain given by

$$\langle [\mathbf{R}(s,t)-\mathbf{R}(s,0)]^2\rangle = 2D_c\frac{a}{L}t + 4\frac{La}{\pi^2}\sum_{p=1}^{\infty}\frac{1}{p^2}\left[1-\exp\left(-\frac{tp^2}{\tau_d}\right)\right] \times \cos^2\left(\frac{p\pi s}{L}\right). \tag{C2}$$

It can be seen from Eq. (C2) for $t > \tau_d$ we get diffusive behavior with a diffusion constant given by

$$D = \frac{1}{3}D_c\frac{a}{L} = \frac{1}{3}\frac{k_BT}{N^2\zeta}\frac{a^2}{b^2}. \tag{C3}$$

APPENDIX D: MEAN-SQUARE DISPLACEMENT OF THE MONOMER

The mean-square displacement of a segment in terms of the normal coordinates is given by

$$\begin{aligned}\langle [\mathbf{R}_n(t)-\mathbf{R}_n(0)]^2\rangle &= \langle [\mathbf{X}_0(t)-\mathbf{X}_0(0)]^2\rangle - 4\left\langle [\mathbf{X}_0(t)-\mathbf{X}_0(0)] \times \sum_{p=1}^{\infty}[\mathbf{X}_p(t)-\mathbf{X}_p(0)]\cos\left(\frac{p\pi n}{N^{2\nu}}\right)\right\rangle \\ &+ \left\langle \left(2\sum_{p=1}^{\infty}[\mathbf{X}_p(t)-\mathbf{X}_p(0)]\cos\left(\frac{p\pi n}{N^{2\nu}}\right)\right)^2\right\rangle.\end{aligned} \tag{D1}$$

Substituting Eq. (7) in Eq. (D1) and using the fact that correlations between different modes vanish, we obtain

$$\langle [\mathbf{R}_n(t)-\mathbf{R}_n(0)]^2\rangle = 6D_ct + 4\sum_{p=1}^{\infty}\langle [\mathbf{X}_p(t) - \mathbf{X}_p(0)]^2\rangle\cos^2\left(\frac{p\pi n}{N^{2\nu}}\right). \tag{D2}$$

Since we are interested in calculating the time taken for a segment to move a mean-square distance of order a^2, we expect this time to be much smaller than the longest relaxation time τ_1. For $t \ll \tau_1$ we have the second term of Eq. (D2) as the dominating term. The second term of Eq. (D2) can be expanded to obtain

$$\begin{aligned}&4\sum_{p=1}^{\infty}[\mathbf{X}_p(t)-\mathbf{X}_p(0)]^2\cos^2\left(\frac{p\pi n}{N^{2\nu}}\right) \\ &= 4\sum_{p=1}^{\infty}\langle \mathbf{X}_p(t)^2\rangle + \langle \mathbf{X}_p(0)^2\rangle \\ &- 8\sum_{p=1}^{\infty}\langle \mathbf{X}_p(t)\cdot\mathbf{X}_p(0)\rangle\cos^2\left(\frac{p\pi n}{N^{2\nu}}\right).\end{aligned} \tag{D3}$$

Using Eq. (B3) we have

$$\langle X_{p\alpha}(t)X_{q\beta}(t)\rangle = 2\frac{k_BT}{\zeta_p}\delta_{\alpha\beta}\delta_{pq} \times \int_{-\infty}^{t} dt_1 \int_{-\infty}^{t} dt_2 \exp\left(\frac{-(t-t_1)}{\tau_p}\right) \times \exp\left(\frac{-(t-t_2)}{\tau_q}\right)\langle f_{p\alpha}(t_1)f_{q\beta}(t_2)\rangle. \tag{D4}$$

This gives $\langle(\mathbf{X}_p(t))^2\rangle = 3k_BT/k_p$ for all t and $\langle \mathbf{X}_p(t)\cdot\mathbf{X}_p(0)\rangle = 3k_BT/k_p \exp(-t/\tau_p)$. Substituting in Eq. (D3) we obtain for $t \ll \tau_1$,

$$\langle[\mathbf{R}_n(t)-\mathbf{R}_n(0)]^2\rangle = 4N^{2\nu}\frac{b^2}{\pi^2}\sum_{p=1}^{\infty}\frac{1}{p^2}\left[1-\exp\left(\frac{-p^2t}{\tau_1}\right)\right] \times \cos^2\left(\frac{p\pi n}{N^{2\nu}}\right). \tag{D5}$$

From Eq. (D5) we can obtain the time taken for an average mean-square displacement of a^2 by a segment as

$$\tau_e = \frac{a^4}{b^2}\frac{\pi}{12}\frac{N^{2(1-2\nu)}\zeta}{k_BT}. \tag{D6}$$

APPENDIX E: FRICTION OF THE HIERARCHICAL TRUNK

Consider, for example, a three tier hierarchical structure of the lattice tree. Hierarchy level 1 consists of a primary trunk of $N^{1/2}$ segments having $N^{1/2}$ primary loops attached to it, each of which contains on an average $N^{1/2}$ beads. Hierarchical level 2 describes the fractal structure of a primary loop, that is, it consists of a secondary trunk of $N^{1/4}$ segments having $N^{1/4}$ secondary loops attached to it, each of which contains on an average $N^{1/4}$ beads. At the hierarchical level 3, each of the secondary loops is described as being composed of a tertiary trunk of $N^{1/8}$ segments having $N^{1/8}$ loops attached to it, each of which contains $N^{1/8}$ beads. We will follow consistently the argument that at any hierarchical level a trunk segment can undergo Brownian reorientational motions only after the loop attached to it has relaxed via its modified Rouse dynamics.

If the friction coefficient of an individual bead is ζ, then the longest Rouse relaxation time of the third hierarchical level loops $\sim N^{1/4}$. This will then manifest itself as the friction coefficient of the segment of the trunk of the third hierarchical level, i.e., $\zeta^{(3)}=N^{1/4}\zeta$. Thus the modified Rouse chain at the third hierarchical level would consist of a chain containing $N^{1/8}$ beads each having a friction coefficient of $N^{1/4}\zeta$. Proceeding similarly to the next higher hierarchical level, the friction coefficient of a trunk segment of hierarchy 2 can be calculated from the longest relaxation time of the modified Rouse chain of hierarchy 3. Thus, $\zeta^{(2)}=(N^{1/8})^2\zeta^{(3)}=N^{1/2}\zeta$. The trunk of the second hierarchy level thus contains $N^{1/4}$ segments each having a friction coefficient given by $N^{1/2}\zeta$. It is then straightforward to calculate the friction coefficient of a segment on the first hierarchical level as being $\zeta^{(1)}=(N^{1/4})^2\zeta^{(2)}=N\zeta$. Generalizing the above argument, it can be shown that for the ith level of hierarchy, $i=1$ being the primary trunk of $N^{1/2}$ segments, the friction coefficient of a trunk segment at that hierarchical level is given by $\zeta^{(i)}=N^{(1/2)^{i-1}}\zeta$.

[1] S. A. Wasserman and N. R. Cozzarelli, Science **232**, 951 (1986).
[2] J. Roovers and P. M. Toporowski, Macromolecules **16**, 843 (1983).
[3] T. C. B. McLeish, *Rheology Reviews*, edited by D. M. Binding and K. Walters (British Society of Rheology, Aberystwyth, Wales, 2003), p. 197.
[4] M. Doi and S. F. Edwards, *The Theory of Polymer Dynamics* (Oxford University Press, New York, 1986).
[5] A. R. Khokhlov and S. K. Nechaev, Phys. Lett. **112A**, 156 (1985).
[6] T. C. B. McLeish and R. G. Larson, J. Rheol. **42**, 81 (1998).
[7] J. Roovers, Macromolecules **21**, 1517 (1988).
[8] G. B. McKenna, G. Hadziioannou, P. Lutz, G. Hild, C. Strazielle, C. Straupe, P. Rempp, and A. J. Kovacs, Macromolecules **20**, 498 (1987).
[9] J. Roovers, Macromolecules **18**, 1359 (1985).
[10] S. Nechaev, *Statistics of Knots and Entangled Random Walks* (World Scientific Publishers, Singapore, 1996).
[11] G. Parisi and N. Sourlas, Phys. Rev. Lett. **46**, 871 (1981).
[12] M. E. Cates and J. M. Deutsch, J. Phys. (Paris) **47**, 2121 (1986).
[13] S. P. Obukhov, M. Rubinstein, and T. Duke, Phys. Rev. Lett. **73**, 1263 (1994).
[14] P. G. de Gennes, J. Chem. Phys. **55**, 572 (1971).
[15] J. Klein, Macromolecules **19**, 105 (1986).
[16] N. C. Karayiannis and V. G. Mavrantzas, Macromolecules **38**, 8583 (2005).
[17] M. Müller, J. P. Wittmer, and M. E. Cates, Phys. Rev. E **53**, 5063 (1996).
[18] M. Müller, J. P. Wittmer, and M. E. Cates, Phys. Rev. E **61**, 4078 (2000).
[19] R. G. Larson, *The Structrue and Rheology of Complex Fluids* (Oxford University Press, New York, 1999).
[20] G. B. McKenna, B. J. Hostetter, N. Hadjichristidia, L. J. Fetters, and D. J. Plazek, Macromolecules **22**, 1834 (1989).
[21] L. J. Fetters, D. J. Lohse, and R. H. Colby, *Physical Properties of Polymers Handbook* (AIP Press, New York, 1996), chap. 24.
[22] L. J. Fetters, D. J. Lohse, and R. H. Colby, *Chain Dimensions and Entanglement Spacings*, http://felix.metsce.psu.edu/rheology/principal/papers_local/MeReview.pdf
[23] K. Hur, R. G. Winkler, and D. Y. Yoon, Macromolecules **39**, 3975 (2006).
[24] S. Brown and G. Szamel, J. Chem. Phys. **109**, 6184 (1998).